MK-Curve improves sensitivity to identify white matter alterations in clinical high risk for psychosis

Fan Zhang[a], **Kang Ik Kevin Cho**[b], **Yingying Tang**[c,d], **Tianhong Zhang**[c], **Sinead Kelly**[b,e], **Maria Di Biase**[b,f], **Lihua Xu**[c,d], **Huijun Li**[g], **Keshevan Matcheri**[e], **Susan Whitfield-Gabrieli**[h,i], **Margaret Niznikiewicz**[j], **William S. Stone**[e], **Jijun Wang**[c,d,*], **Martha E. Shenton**[b,f], **Ofer Pasternak**[a,b,*]

[a]Department of Radiology, Brigham and Women's Hospital, Harvard Medical School, Boston, MA, USA

[b]Department of Psychiatry, Brigham and Women's Hospital, Harvard Medical School, Boston, MA, USA

[c]Shanghai Key Laboratory of Psychotic Disorders, Shanghai Mental Health Center, Shanghai Jiao Tong University School of Medicine, Shanghai, China

[d]Brain Science and Technology Research Center, Shanghai Jiao Tong University, Shanghai, China

[e]The Massachusetts Mental Health Center, Public Psychiatry Division, Beth Israel Deaconess Medical Center, and Harvard Medical School, Boston, MA, USA

[f]Melbourne Neuropsychiatry Centre, Department of Psychiatry, The University of Melbourne and Melbourne Health, Carlton South, Victoria, Australia

[g]Department of Psychology, Florida A&M University, Tallahassee, FL,USA

[h]Department of Psychology, Northeastern University, Boston, MA, USA

[i]The McGovern Institute for Brain Research and the Poitras Center for Affective Disorders Research, Massachusetts Institute of Technology, Cambridge, MA, USA

[j]The Department of Psychiatry, Veterans Affairs Boston Healthcare System, Brockton Division, Brockton, MA, USA

Abstract

Diffusion kurtosis imaging (DKI) is a diffusion MRI approach that enables the measurement of brain microstructural properties, reflecting molecular restrictions and tissue heterogeneity. DKI parameters such as mean kurtosis (MK) provide additional subtle information to that provided by popular diffusion tensor imaging (DTI) parameters, and thus have been considered useful to detect white matter abnormalities, especially in populations that are not expected to show severe brain pathologies. However, DKI parameters often yield artifactual output values that are outside of the biologically plausible range, which diminish sensitivity to identify true microstructural changes. Recently we have proposed the mean-kurtosis-curve (MK-Curve) method to correct voxels with implausible DKI parameters, and demonstrated its improved performance against other approaches that correct artifacts in DKI. In this work, we aimed to evaluate the utility of the MK-Curve method to improve the identification of white matter abnormalities in group comparisons. To do so, we compared group differences, with and without the MK-Curve correction, between 115 individuals at clinical high risk for psychosis (CHR) and 93 healthy controls (HCs). We also compared the correlation of the corrected and uncorrected DKI parameters with clinical characteristics. Following the MK-curve correction, the group differences had larger effect sizes and higher statistical significance (i.e., lower p-values), demonstrating increased sensitivity to detect group differences, in particular in MK. Furthermore, the MK-curve-corrected DKI parameters displayed stronger correlations with clinical variables in CHR individuals, demonstrating the clinical relevance of the corrected parameters. Overall, following the MK-curve correction our analyses found widespread lower MK in CHR that overlapped with lower fractional anisotropy (FA), and both measures were significantly correlated with a decline in functioning and with more severe symptoms. These observations further characterize white matter alterations in the CHR stage, demonstrating that MK and FA abnormalities are widespread, and mostly overlap. The improvement in group differences and stronger correlation with clinical variables suggest that applying MK-curve would be beneficial for the detection and characterization of subtle group differences in other experiments as well.

1. Introduction

Diffusion kurtosis imaging (DKI) (Jensen et al., 2005) is a diffusion MRI (dMRI) approach to characterize non-Gaussian water molecule diffusion that reflects microstructural changes in molecular restrictions and tissue heterogeneity (Cheung et al., 2009; Steven et al., 2014; Tabesh et al., 2011). Non-Gaussian diffusion may arise in the brain when diffusion is restricted by barriers, such as cell membranes and organelles, and also when microstructural compartments with distinct diffusion properties reside in the same voxel (Fieremans et al., 2011; Westin et al., 2016; Yang et al., 2012). Since DKI is a clinically feasible extension of diffusion tensor imaging (DTI) (Basser et al., 1994), it characterizes general shape and size parameters akin to standard DTI, such as fractional anisotropy (FA) and mean diffusivity (MD) Pierpaoli and Basser (1996), but in addition it estimates kurtosis-specific parameters that quantify the non-Gaussian contribution to the diffusion profile, including mean kurtosis (MK), axial kurtosis (AK) and radial kurtosis (RK) (Hui et al., 2008; Jensen et al., 2005; Lu et al., 2006).

In the white matter, kurtosis parameters (e.g., MK, AK, and RK) have been suggested to indicate the complexity of the brain's microstructural environment (Steven et al., 2014).

Since non-Gaussian contributions can originate from restricted diffusion, changes in kurtosis parameters are thought to better reflect changes to the microstructure of the fiber bundles themselves, e.g., to the barriers posed by the myelin sheath, when compared to DTI measures. Other microstructural differences (e.g., dispersion and density of fibers), as well as partial volume effects, which reflect more on the organization of fiber bundles could also cause changes in kurtosis parameters.

While DKI parameters are useful for identifying subtle microstructural differences, there are technical difficulties that limit the accuracy of DKI. Specifically, DKI parameters calculated directly from dMRI data, with no additional processing, often have implausible values, which are values outside of the expected range within biological tissue (Jensen et al., 2005; Shaw and Jensen, 2017; Tabesh et al., 2011; Zhang et al., 2019a). In MK images, implausible values often appear as very dark or very bright voxels within brain tissue, which no longer truly represent any microstructural effects (e.g., negative MK values). The number of voxels with implausible values in a typical MK map is considerable (see for example Fig. 2b), and is especially high in clinical acquisitions (Zhang et al., 2019a). If not corrected, implausible values introduce large biases and increased variability in any resulting DKI parameters. Biases and increased variability can in turn lead to challenges in interpreting the findings, and detecting between-group differences (Shaw and Jensen, 2017). Recently, we introduced the mean-kurtosis-curve (MK-Curve) method, as a robust approach to correct implausible DKI parameter values (Zhang et al., 2019a). MK-curve was validated on synthetic phantom, ex-vivo phantom, and in-vivo brain dMRI data, and was found to correct more implausible voxels than other available methods (Zhang et al., 2019a). The method generates a curve for each voxel that explains how MK values change as a function of the b0 signal. The shape of the resulting curve defines ranges of b0 values that generate implausible MK values, enabling detection and correction of implausible DKI voxels by projecting out-of-range b0 values to the plausible range. By correcting voxels with implausible values, MK-Curve intends to improve the accuracy of DKI measures, and therefore to re-enable assigning a biological interpretation to those voxels.

In this work we demonstrate that applying MK-curve to correct voxels with implausible MK values increases the sensitivity of DKI to identify white matter alteration. To evaluate this improvement we test for group differences in DKI and MK-curve corrected DKI measures between healthy controls and individuals at clinical high risk of developing psychosis (CHR). DKI measures have been found useful for the identification and characterization of neurological changes in psychosis (Cho et al., 2019; Kochunov et al., 2016; Pasternak et al., 2018; Ramani et al., 2007; Zhu et al., 2016, 2015), but have not yet been applied to CHR. Previous dMRI studies in CHR repeatedly identified subtle white matter abnormalities (Bloemen et al., 2010; Clemm von Hohenberg et al., 2014; Karlsgodt et al., 2009; Peters et al., 2010, 2009; Tang et al., 2019), which were explained as likely having a neurodevelopmental root contributing to the etiology of psychosis. These studies help establish the presence of white matter abnormalities in CHR populations, but since they are mostly based on standard DTI analysis, they provide limited information about the microstructural properties underlying these abnormalities. Therefore, more advanced dMRI methods are required to characterize further their microstructural properties (Karlsgodt, 2020; Pasternak et al., 2018), which may shed light on their origin and cellular basis. To

increase the homogeneity of the CHR group while maintaining a sufficiently large group to identify subtle differences we include only those CHR individuals who were not medicated, and that did not develop psychosis within a one-year follow-up period. Therefore, the group difference in dMRI measures between this CHR chort and HCs is expected to have small effect sizes and could be amplified by improved sensitivity following the MK-curve correction. We compare the DKI parameters (including FA and MK) calculated directly from the dMRI data to those after correction for implausible values using the MK-Curve method (Zhang et al., 2019a). For each of the calculated DKI parameters, tract-based spatial statistics (TBSS) (Smith et al., 2006) is performed to identify white matter differences in a large sample of CHR subjects compared to healthy controls (HCs). Group differences of DKI parameters averaged across the white matter skeleton and on a voxel-wise level are reported. Correlation analyses are used to test for associations between the DKI parameters and clinical characteristics.

2. Methods

2.1. Participants

Participants in this study are 115 help-seeking individuals from the Shanghai At Risk for Psychosis (SHARP) program (Shanghai Mental Health Center, Shanghai, China) that were recruited at their first outpatient assessment, and 93 age and gender matched healthy control (HC) subjects that were recruited through online advertisements. The mean intervals between recruitment and MRI scan were 2.5 days (SD = 7.7). All recruited subjects in the CHR group met CHR criteria, defined by the Chinese version of the Structured Interview for Prodromal Syndromes (SIPS) and the Scale of Prodromal Symptoms (SOPS) (Zheng et al., 2012), administered by a senior psychiatrist (T.Z and L.X.) (Zhang et al., 2015, 2014).

Exclusion criteria at study entry for all participants included head injury with loss of consciousness of any duration; any history of substance use, neurological disease, severe somatic diseases; IQ below 70; and dementia. Control subjects were additionally excluded if they met the criteria for a psychotic disorder or a clinical high-risk syndrome (determined by the SIPS) or any other mental disorder defined by DSM-IV. Exclusion criteria for CHR included prior treatment with psychotropic medication such as antipsychotics, antidepressants or benzodiazepines. In the current study we did not include CHR subjects who had developed psychosis within a 1-year follow-up evaluation (additional 16 subjects that were excluded). These subjects were excluded to simplify the clinical heterogeneity of the CHR group at test, and are saved for future longitudinal studies that will focus on clinical trajectories and outcomes.

On all subjects, and as part of the SIPS evaluation, the Global Assessment of Functioning Scale (GAF) was administered to evaluate a functioning score for the time of recruitment, and retrospectively for the 12 months prior to the initial assessment. Functional decline, which is required for the SIPS definition of CHR was calculated as the drop in the current GAF score at the time of assessment compared with the subject's highest estimated GAF score in the 12 months prior to the initial assessment (Tang et al., 2019; Zhang et al., 2015, 2014). We also investigated additional symptom measures that are assessed as part of SIPS. These were a total of 19 variables, including 5 positive symptoms, 6 negative symptoms, 4

disorganization symptoms, and 4 general symptoms. We note that while SIPS was administered by two highly trained psychiatrists, for the current study we did not have data that allowed us to assess inter-rater reliability in SIPS-derived scores.

A summary of the demographics of all CHR and HC individuals is presented in Table 1. All individuals passed imaging quality control evaluation (see Section 2.2). We note that 39 of the CHR and 50 of the HC individuals were included in a previous dMRI study (Tang et al., 2019). The study protocol and consent form were reviewed and approved by the local ethics committees. Written informed consent was obtained from all participants.

2.2. MRI data acquisition and image preprocessing

All participants underwent MRI scanning at the Shanghai Mental Health Center using a 3-T Verio scanner (Siemens, Munich) with a 32-channel head coil. The acquisition parameters used for the dMRI data were TE = 109 ms, TR = 15800 ms, phase partial Fourier = 6/8, and voxel size = $2 \times 2 \times 2$ mm^3. A total of 74 images were acquired for each subject, including 5 baseline images with $b = 0$ s/mm^2, 3 diffusion-weighted (DW) images with $b = 200$ s/mm^2, 5 DW images with $b = 500$ s/mm^2, and 30 DW images with $b = 1000$ s/mm^2, and 30 DW images at 3000 s/mm^2. Scanning parameters and acquisitions at the Shanghai Mental Health Center were supervised by members of the Psychiatry Neuroimaging Laboratory (PNL) at Brigham and Women's Hospital (BWH), with visits to Shanghai and ongoing communication with the chief technical scientist (Y.T.) in Shanghai. All data processing was performed at the PNL.

The dMRI data was preprocessed using in-house data processing pipeline (github.com/pnlbwh/pnlpipe), including brain masking using the SlicerDMRI extension (dmri.slicer.org) (Norton et al., 2017; Zhang et al., 2020b) in 3D Slicer (www.slicer.org) and eddy current-induced distortion correction, outlier replacement and motion correction using Eddy (Andersson et al., 2016; Andersson and Sotiropoulos, 2016), FSL (Jenkinson et al., 2012). Motion parameters were derived from the FSL permutations and compared between the CHR and HC subjects, where no significant differences were identified ($p = 0.52$). All dMRI scans included in the study passed quality control, which included visual inspection of the raw data and visual inspection of the output images by trained raters at the PNL.

2.3. Calculation of DKI and DTI parameters

For each of the preprocessed dMRI scans, we computed the following DKI-based parameters: FA$_{DKI}$ and MK$_{DKI}$, which were computed using the standard DKI model fit (Tabesh et al., 2011) without any correction for implausible values (Section 2.3.1), and FA$_{MKC}$ and MK$_{MKC}$, which were corrected for the implausible values using MK-curve (Zhang et al., 2019a) (Section 2.3.2). As a comparison, we also computed a DTI-based FA parameter, i.e., FA$_{DTI}$ (Section 2.3.3). See Fig. 1 for an overview of the compared parameters.

2.3.1. DKI model fit for computation of FA$_{DKI}$ and MK$_{DKI}$—The DKI model (Tabesh et al., 2011) describes the dMRI signal in each voxel as a combination of a diffusion tensor and a kurtosis tensor, reflecting the Gaussian and excessive non-Gaussian water

molecule diffusion, respectively. A non constrained weighted linear least square (WLLS) fitting (Veraart et al., 2013) was applied to compute the diffusion tensor and the kurtosis tensor ("*dki_fit.m*" and "*dki_parameters.m*" from github.com/NYU-DiffusionMRI/ DESIGNER). From the estimated diffusion tensor, we calculated FA_{DKI}, and from the estimated kurtosis tensor, we computed MK_{DKI} (Tabesh et al., 2011).

2.3.2. MK-Curve correction for computation of FA_{MKC} and MK_{MKC}—MK-Curve is a continuous plot that shows the dependency of MK on variations in the b0 signal. It has been used to robustly correct implausible DKI and DTI parameter values (Zhang et al., 2019a) and to improve brain tissue segmentation (Zhang et al., 2020a). An MK-Curve is generated for each voxel by replacing the original b0 value with a range of synthetic values, while not altering any of the diffusion-weighted signals, and then calculating and plotting MK for each signal realization (github.com/zhangfanmark/MK-Curve). The MK-Curve has a similar shape for all brain tissue/regions (Fig. 2a): Looking from right to left, and starting from the maximal synthetic b0, as the synthetic b0 value decreases, the MK values steadily increase until reaching a peak (i.e., *max-MK*), which we define as a characteristic b0 value and call *max-MK b0*. The curve then continues with a sharp decrease in the MK value, which crosses MK = 0 (i.e., *zero-MK*) at another characteristic b0 value that we define as *zero-MK b0*. Then, when the synthetic b0 value is further reduced, the MK value enters an unstable phase where MK fluctuates dramatically, often reaching extreme low and high values. This range of b0 values was found to include the vast majority of implausible MK values (see (Zhang et al., 2019a) for details). By comparing the original b0 with the two characteristic b0 values (i.e., zero-MK b0 and max-MK b0), the MK-curve enables detection and correction of implausible voxels by projecting out-of-range b0 values to a new value that is within the plausible range. The corrected DKI parameters, i.e., FA_{MKC} and MK_{MKC}, are then those that were fitted from the dMRI data with the new b0 value. The corrected parameter maps eliminate the vast majority of implausible values (e.g. comparing dark voxels in the original MK map and bright voxels in the original FA map with the corrected MK and FA maps in Fig. 2b). At the same time, the MK-Curve method minimally changed the dMRI data by slightly changing only the b0 signals of those voxels that were detected to have implausible MK values (see Fig. 2a).

2.3.3. DTI model fit for computation of FA_{DTI}—We also applied DTI by a nonlinear fit estimation of a diffusion tensor in each voxel, and computed FA_{DTI} (Pierpaoli and Basser, 1996). For the DTI model fit, we only included $b = 0$ and $b = 1000$ s/mm^2 shells.

2.4. Statistical comparison

We used tract based spatial statistics (TBSS) (Smith et al., 2006) to generate a white matter skeleton and calculate statistical differences of dMRI measures on the skeleton between the CHR and HC groups. The FA_{DTI} images of all subjects were registered to the Enhancing Neuro Imaging Genetics through Meta-Analysis (ENIGMA) FA template, and projected onto the ENIGMA predefined white matter skeleton (Thompson et al., 2014). The FA_{DTI}-based registration transformation was then applied to the other dMRI parameter maps (i.e., FA_{DKI}, MK_{DKI}, FA_{MKC} and MK_{MKC}) and they were subsequently projected onto the same white matter skeleton.

We then performed group comparisons using two different levels of analyses: averaged-skelton analysis to identify group differences over the entire white matter skeleton (Section 2.4.1), and voxel-wise analysis to identify the spatial extent of group differences (Section 2.4.2).

2.4.1. Averaged skeleton analysis—For the first level of analysis, all dMRI parameter values were averaged across the white matter skeleton in order to identify differences between groups that are spatially diffuse. First, to assess the impact of the MK-curve correction on the dMRI values themselves, we performed a paired t-test to compare FA and MK before and after correction (FA_{DKI} versus FA_{MKC}, and MK_{DKI} versus MK_{MKC}). Second, to assess the impact of the MK-curve correction on the ability to identify group differences, for each parameter, a generalized linear model (GLM) was constructed to compare the CHR and HC groups, where the average dMRI parameter was the dependent variable, group was a predictor variable, and age and gender were covariates.

Linear correlation analyses (controlled for age and sex) were used to test for associations between average dMRI parameter values and functional decline in both CHR and HC. A comparison of the correlation coefficient of the diffusion measures before and after MK-curve correction (FA_{DKI} versus FA_{MKC}, and MK_{DKI} versus MK_{MKC}) was conducted using a Fisher r-to-z transformation test Williams (1959). For correlations with additional symptom measures see Supplementary Experiment 1.

In all averaged skeleton analyses significant group differences were defined as those with $p < 0.05$, and Cohen's d measure was computed to assess the effect size for differences between group means.

2.4.2. Voxel-wise analysis—In the second level of analysis, a GLM was fitted to each voxel on the white matter skeleton to identify the spatial extent of group differences. This analysis was performed using the permutation test in the randomize tool of FSL (Winkler et al., 2014). Threshold-free cluster enhancement (TFCE) Smith and Nichols (2009) was applied to control for family-wise errors, with a significance threshold (TFCE modified) of $p < 0.05$. Age and gender were included as covariates. Anatomical locations of the identified voxels were identified using the ICBM-DTI-81 atlas (Mori et al., 2005).

Similar to the averaged-skeleton analysis, we performed linear correlation analyses (controlling for age and sex) between average parameter value over the significant voxels and the functional decline measure in both CHR and HC, and considered $p < 0.05$ as significant. We also utilized additional data from the Human Connectome Project (Glasser et al., 2013) to evaluate test-retest reliability of the MK and FA measures before and after MK-curve correction (See Supplementary Experiment 2).

3. Results

3.1. Averaged skeleton analysis

MK-curve corrected measures had significantly lower FA (p<0.001, Cohen's d = 5.50, in HC; $p < 0.001$, Cohen's d = 5.38, in CHR; compare FA_{DKI} with FA_{MKC} in Fig. 3), and

significantly higher MK ($p < 0.001$, Cohen's d = 5.50, in HC; $p < 0.001$, Cohen's d = 5.41, in CHR; compare MK_{DKI} and MK_{MKC} in Fig. 3) when averaged across the whole white matter skeleton. Comparing the average dMRI measures between CHR and HC, we found that the CHR group had lower values in both FA-based (FA_{DTI}, FA_{DKI}, and FA_{MKC}) and MK-based (MK_{DKI} and MK_{MKC}) parameters (Fig. 3). When comparing before and after correction (Fig. 3), the MK-curve corrected parameters (FA_{MKC} or MK_{MKC}) had higher effect sizes (Cohen's d) for group differences and lower p-value than the corresponding non-corrected (FA_{DKI} or MK_{DKI}) parameters, although, FA_{MKC} was the only parameter to show a statistical significant group difference ($p = 0.013$). Following the MK-curve correction, the FA_{MKC} parameter had a slightly stronger correlation coefficient ($r = -0.268$; $p = 0.004$) than the FA_{DKI} parameter before correction ($r = -0.265$; $p = 0.005$), and both had a stronger correlation coefficient than the FA_{DTI} parameter ($r = -0.241$; $p = 0.01$) (Fig. 4). The MK parameter was significantly correlated with clinical decline following the MK-curve correction (i.e., MK_{MKC}, $r = -0.261$; $p = 0.005$) but not before the correction (i.e., MK_{DKI} $r = -0.106$; $p = 0.264$), although a Fisher r-to-z transformation test did not show a significant difference ($z = 1.191$; $p = 0.117$) between the two correlation coefficients (Fig. 4). Similar results, i.e., stronger correlation with dMRI measures following MK-curve correction were found for the symptom measures (see Supplementary Experiment 1). There were no significant correlations between dMRI and clinical measures within HC (Fig. 4), both before and after MK-curve correction.

3.2. Voxel-wise analysis

The comparison of the voxel by voxel group differences in dMRI measures between HC and CHR identified voxels with significantly lower values in the CHR group for all five dMRI parameters. There were no voxels with significantly higher values. The number of voxels with significant group difference was higher following the MK-Curve correction (Fig. 5 and Table 2), in particular for the MK parameter (MK_{DKI} vs MK_{MKC}). The locations implicated by the FA_{DKI} and FA_{MKC} maps were similar, with a large spatial overlap between the maps (Fig. 5). For the MK maps, most voxels with significantly lower MK_{DKI} had also significantly lower MK_{MKC}, although the significant MK_{MKC} voxels were further widespread across the white matter skeleton (Fig. 5 and see also Supplementary Figure S1 for the effect on each ROI in the ICBM-DTI-81 atlas). Similarly to the averaged skeleton analysis, calculating the correlation with functional decline over those voxels that showed significant group difference, demonstrated stronger correlation for the MK-curve corrected parameters compared with the uncorrected parameters (Supplementary Figure S2). Finally, MK-curve corrected measures had better test-retest reliability than uncorrected DKI measures when averaged across the entire skeleton, and also across individual white matter ROIs (Supplementary Experiment 2).

4. Discussion

In this work, we demonstrate that applying the MK-curve method improves identification of DKI abnormalities in the white matter by comparing a population of CHR individuals with HC. Following the MK-curve correction, the group differences had higher effect sizes and statistical significance (i.e., lower p values), demonstrating increased sensitivity to group

differences. Furthermore, the MK-curve-corrected DKI parameters had stronger correlation with clinical variables in CHR individuals, demonstrating the clinical relevance of the corrected parameters. Overall, our analyses found lower FA and lower MK in the CHR individuals, which is consistent with previous dMRI findings that were reported across the psychosis spectrum. Following the MK-curve correction, we found that both FA and MK abnormalities are widespread and are overlapping.

The MK-curve correction, both averaged across the white matter skeleton and in voxel-wise analyses, increased sensitivity to identify group differences and also improved the clinical relevance, demonstrating stronger correlation with clinical characteristics. Although direct statistical comparisons did not demonstrate a significant change in the correlation coefficients themselves following the MK-curve correction which means that the interpretation of the underlying biology did not substantially change, the improvement in effect size and correlation coefficients did affect the inferred significance of some of the correlation tests. For example, the correlation of MK with functional decline was not significant prior to the MK-curve correction, and significant after correction. This serves as a demonstration for how potentially small improvement in the accuracy of measures could change the conclusion of studies, especially when the effect under study is subtle or small. Without the MK-correction, the measures include many implausible values, which do not fully reflect the actual microstructural properties of the white matter (as illustrated in Supplementary Experiment 3). This is particularly obvious for the MK measure that is highly affected by implausible values. Instead, the implausible parameters represent image artifacts that are not group specific, and thus diminish real group differences. The causes for implausible DKI parameter values include various image artifacts such as Gibbs ringing (Perrone et al., 2015; Veraart et al., 2016), noise and subject motion (Shaw and Jensen, 2017; Tabesh et al., 2011). These factors typically have greater effect on kurtosis parameters than on DTI parameters (Perrone et al., 2015; Shaw and Jensen, 2017; Tabesh et al., 2011), corresponding to our observation that correcting implausible values mostly improved the effect size and correlation coefficients of the MK values. In addition we also show that the test retest reliability of the MK and FA measures are improved following the MK-curve correction. Taken together, our analyses demonstrate the utility and importance of the MK-curve correction for statistical analyses of DKI-based parameters.

Beyond the technical implications, our analyses also add to the understanding of microstructural properties of white matter abnormalities in CHR. Our statistical comparisons overall suggested significantly lower FA and MK in the CHR individuals, with widespread changes in the white matter, including the corpus callosum (including the tapetum), the bilateral posterior thalamic radiation and the fornix, which are consistent with the locations implicated in previous dMRI studies of CHR individuals (Baumann et al., 2016; Carletti et al., 2012; Clemm von Hohenberg et al., 2014). Most of the previous dMRI studies in CHR apply DTI-based tissue modeling and report reduced FA (Bloemen et al., 2010; Carletti et al., 2012; Clemm von Hohenberg et al., 2014; Karlsgodt et al., 2009; Peters et al., 2009). However, DTI cannot identify the biological compartment responsible for the changes in FA, since FA is sensitive to multiple biological and geometrical effects that may not provide a good approximation of white matter integrity (Jones et al., 2013). More recent studies that applied compartmental models suggested that the changes in FA in CHR likely originate

from a cellular compartment, rather than from an extracellular compartment (Tang et al., 2019; Wang et al., 2016). The widespread and overlapping non-gaussian (MK) and gaussian (FA) differences, that we found in the current study, further support the accumulating evidence of white matter abnormalities that precede psychosis. The uncorrected MK may suggest that there are specific brain areas with WM pathology that affects MK and is additional to a more widespread pathology that affects FA. However, the higher sensitivity to identify MK abnormalities revealed that the MK differences overlap with the FA differences, suggesting that different aspects of potentially the same underlying processes may affect both measures. These white matter abnormalities could be driven by changes in the microstructural organization of the cellular domain, such as alterations in cellular heterogeneity and/or alterations in cellular boundaries that cause restricted diffusion and that also affect anisotropy. These abnormalities are aligned with previous hypotheses suggesting that early pathologies, likely rooted in neurodevelopment, affect the composition of the white matter in CHR (Bloemen et al., 2010; Clemm von Hohenberg et al., 2014; Karlsgodt et al., 2009; Peters et al., 2010, 2009; Tang et al., 2019). Although, we note that our analyses here can not directly infer a neurodevelopmental source, also since much like other dMRI measures, MK is not specific to intracellular changes and may be affected by regions of complex fiber architecture and other partial volume effects. Alternatively, these cellular changes may reflect progressive changes; better differentiation between these etiological hypotheses would require future longitudinal and multi-modal or multi compartmental analyses.

Our findings should also be evaluated with respect to the unique cohort that was studied here, i.e., CHR that are not medicated, and that did not develop psychosis within one-year follow-up period. We chose to focus on non-medicated subjects and those that did not develop psychosis in order to maximize group homogeneity. Accordingly, subjects included in this cohort were all suffering from attenuated psychotic symptoms (as opposed to genetic risk), and the fact that both the (corrected) MK and FA measures were significantly correlated with decline in functioning and clinical symptoms further demonstrate the relevance of white matter microstructure. In the current study, we did not include subjects who eventually developed psychosis, and therefore we cannot comment on the utility of DKI measures as biomarkers of conversion. However, CHR subjects regardless of their outcome are considered as part of the same continuum (Addington et al., 2020; Carpenter, 2017; Lin et al., 2015), where events and environmental effects that occur following a baseline evaluation could be more determinant regarding clinical outcomes. The fact that the MK-curve correction improved both sensitivity and the correlation with clinical measures suggests that future studies that will include a wider range of clinical outcomes would benefit from studying MK-curve corrected DKI parameters. In the current study, there was not a significant difference in the female/male proportions between HC and CHR ($p = 0.09$, see Table 1). However, since the groups were not perfectly matched, sex was included as a covariate in the statistical comparisons. The study of sex differences and interaction of diffusion meausres with sex in CHR is left for future work.

Since previous studies did not apply DKI in a CHR population, it is informative to compare our results with other DKI studies of psychosis. Such studies typically report that MK abnormalities are implicated in different locations than the locations of FA abnormalities

(Docx et al., 2017; McKenna et al., 2019; Narita et al., 2016; Zhu et al., 2015), suggesting that MK and FA may potentially identify two different pathologies related to psychosis. Our results showed large overlaps between MK and FA, which is not in agreement with the previous studies in psychosis. We note, however, that similarly to the previous studies that did not apply MK-Curve, the uncorrected MK had a much smaller overlap with FA in our study, which may suggest that not correcting implausible MK in the previous studies limited the spatial extent of the MK abnormalities.

To conclude, in this paper we demonstrated the utility of applying the MK-curve correction to improve effect sizes in group comparisons and to improve the clinical relevancy of DKI derived white matter parameters. While we demonstrated these effects in a specific population of CHR, the application of MK-curve could be useful to any statistical analysis of DKI derived parameters in other populations as well. DKI studies have already demonstrated interesting findings in characterization of neurological changes in aging (Falangola et al., 2008; Grinberg et al., 2017) and in rodent brain maturation (Cheung et al., 2009), as well as in neurological disorders, such as brain tumors (Raab et al., 2010), Alzheimer's disease (Benitez et al., 2014), and traumatic brain injury (Zhuo et al., 2012). Since the MK-Curve method eliminates the effect of implausible DKI parameters (Zhang et al., 2019a), it is expected that MK-curve would improve the utility of DKI measures in such populations as well.

Data and code availability statement

The MRI datasets of the subjects under study belong to our onsite MR data, which cannot be made publicly available because public availability would compromise participant confidentiality or participant privacy.

The code of the method described in the paper is available online, as stated in the paper.

Supplementary Material

Refer to Web version on PubMed Central for supplementary material.

Acknowledgement

References

Addington J, Farris M, Devoe D, Metzak P, 2020 Progression from being at-risk to psychosis: next steps. npj Schizophrenia 6, 27. [PubMed: 33020486]

Andersson JLR, Graham MS, Zsoldos E, Sotiropoulos SN, 2016 Incorporating outlier detection and replacement into a non-parametric framework for movement and distortion correction of diffusion MR images. Neuroimage 141, 556–572. [PubMed: 27393418]

Andersson JLR, Sotiropoulos SN, 2016 An integrated approach to correction for off-resonance effects and subject movement in diffusion MR imaging. Neuroimage 125, 1063–1078. [PubMed: 26481672]

Basser PJ, Mattiello J, LeBihan D, 1994 MR diffusion tensor spectroscopy and imaging. Biophys. J 66, 259–267. [PubMed: 8130344]

Baumann PS, Griffa A, Fournier M, Golay P, Ferrari C, Alameda L, Cuenod M, Thiran J-P, Hagmann P, Do KQ, Conus P, 2016 Impaired fornix-hippocampus integrity is linked to peripheral glutathione peroxidase in early psychosis. Transl. Psychiatry 6, e859. [PubMed: 27459724]

Benitez A, Fieremans E, Jensen JH, Falangola MF, Tabesh A, Ferris SH, Helpern JA, 2014 White matter tract integrity metrics reflect the vulnerability of late-myelinating tracts in Alzheimer's disease. NeuroImage 4, 64–71. [PubMed: 24319654]

Bloemen OJN, de Koning MB, Schmitz N, Nieman DH, Becker HE, de Haan L, Dingemans P, Linszen DH, van Amelsvoort TAMJ, 2010 White-matter markers for psychosis in a prospective ultra-high-risk cohort. Psychol. Med 40, 1297–1304. [PubMed: 19895720]

Carletti F, Woolley JB, Bhattacharyya S, Perez-Iglesias R, Fusar Poli P, Valmaggia L, Broome MR, Bramon E, Johns L, Giampietro V, Williams SCR, Barker GJ, McGuire PK, 2012 Alterations in white matter evident before the onset of psychosis. Schizophr. Bull 38, 1170–1179. [PubMed: 22472474]

Carpenter WT, 2017 Clinical high risk controversies and challenge for the experts. Schizophr. Bull 44, 223–225.

Cheung MM, Hui ES, Chan KC, Helpern JA, Qi L, Wu EX, 2009 Does diffusion kurtosis imaging lead to better neural tissue characterization? A rodent brain maturation study. NeuroImage 45, 386–392. [PubMed: 19150655]

Cho KIK, Kwak YB, Hwang WJ, Lee J, Kim M, Lee TY, Kwon JS, 2019 Microstructural changes in higher-order nuclei of the thalamus in patients with first-episode psychosis. Biol. Psychiatry 85, 70–78. [PubMed: 29961564]

Clemm von Hohenberg C, Pasternak O, Kubicki M, Ballinger T, Vu M-A, Swisher T, Green K, Giwerc M, Dahlben B, Goldstein JM, Woo T-UW, Petryshen TL, Mesholam-Gately RI, Woodberry KA, Thermenos HW, Mulert C, McCarley RW, Seidman LJ, Shenton ME, 2014 White Matter Microstructure in individuals at clinical high risk of psychosis: a whole-brain diffusion tensor imaging study. Schizophr. Bull 40, 895–903. [PubMed: 23737549]

Docx L, Emsell L, Van Hecke W, De Bondt T, Parizel PM, Sabbe B, Morrens M, 2017 White matter microstructure and volitional motor activity in schizophrenia: a diffusion kurtosis imaging study. Psychiatry Res. Neuroimaging 260, 29–36. [PubMed: 28012424]

Falangola MF, Jensen JH, Babb JS, Hu C, Castellanos FX, Di Martino A, Ferris SH, Helpern JA, 2008 Age-related non-Gaussian diffusion patterns in the prefrontal brain. J. Magnetic Resonance Imaging 28, 1345–1350.

Fieremans E, Jensen JH, Helpern JA, 2011 White matter characterization with diffusional kurtosis imaging. Neuroimage 58, 177–188. [PubMed: 21699989]

Glasser MF, Sotiropoulos SN, Wilson JA, Coalson TS, Fischl B, Andersson JL, Xu J, Jbabdi S, Webster M, Polimeni JR, Van Essen DC, Jenkinson MWU-Minn HCP Consortium, 2013 The minimal preprocessing pipelines for the human connectome project. Neuroimage 80, 105–124. [PubMed: 23668970]

Grinberg F, Maximov II, Farrher E, Neuner I, Amort L, Thönneßen H, Oberwelland E, Konrad K, Shah NJ, 2017 Diffusion kurtosis metrics as biomarkers of microstructural development: a comparative study of a group of children and a group of adults. NeuroImage 144, 12–22. [PubMed: 27639358]

Hui ES, Cheung MM, Qi L, Wu EX, 2008 Towards better MR characterization of neural tissues using directional diffusion kurtosis analysis. NeuroImage 42, 122–134. [PubMed: 18524628]

Jenkinson M, Beckmann CF, Behrens TEJ, Woolrich MW, Smith SM, 2012 FSL. Neuroimage 62, 782–790. [PubMed: 21979382]

Jensen JH, Helpern JA, Ramani A, Lu H, Kaczynski K, 2005 Diffusional kurtosis imaging: the quantification of non-gaussian water diffusion by means of magnetic resonance imaging. Magnetic Resonance Med. 53, 1432–1440.

Jones DK, Knösche TR, Turner R, 2013 White matter integrity, fiber count, and other fallacies: the do's and don'ts of diffusion MRI. Neuroimage 73, 239–254. [PubMed: 22846632]

Karlsgodt KH, 2020 White Matter Microstructure across the Psychosis Spectrum. Trends Neurosci 43, 406–416. [PubMed: 32349908]

Karlsgodt KH, Niendam TA, Bearden CE, Cannon TD, 2009 White matter integrity and prediction of social and role functioning in subjects at ultra-high risk for psychosis. Biol. Psychiatry 66, 562–569. [PubMed: 19423081]

Kochunov P, Rowland LM, Fieremans E, Veraart J, Jahanshad N, Eskandar G, Du X, Muellerklein F, Savransky A, Shukla D, Sampath H, Thompson PM, Hong LE, 2016 Diffusion-weighted imaging uncovers likely sources of processing-speed deficits in schizophrenia. Proc. Natl. Acad. Sci. U. S. A 113, 13504–13509. [PubMed: 27834215]

Lin A, Wood SJ, Nelson B, Beavan A, McGorry P, Yung AR, 2015 Outcomes of nontransitioned cases in a sample at ultra-high risk for psychosis. AJP 172, 249–258.

Lu H, Jensen JH, Ramani A, Helpern JA, 2006 Three-dimensional characterization of non-gaussian water diffusion in humans using diffusion kurtosis imaging. NMR Biomed. 19, 236–247. [PubMed: 16521095]

McKenna FF, Miles L, Babb JS, Goff DC, Lazar M, 2019 Diffusion kurtosis imaging of gray matter in schizophrenia. Cortex 121, 201–224 [PubMed: 31629198]

Mori S, Wakana S, Van Zijl PCM, Nagae-Poetscher LM, 2005 MRI atlas of human white matter. Elsevier.

Narita H, Tha KK, Hashimoto N, Hamaguchi H, Nakagawa S, Shirato H, Kusumi I, 2016 Mean kurtosis alterations of cerebral white matter in patients with schizophrenia revealed by diffusion kurtosis imaging. Prog. Neuropsychopharmacol. Biol. Psychiatry 71, 169–175. [PubMed: 27495358]

Norton I, Essayed WI, Zhang F, Pujol S, Yarmarkovich A, Golby AJ, Kindlmann G, Wassermann D, Estepar RSJ, Rathi Y, Pieper S, Kikinis R, Johnson HJ, Westin C-F, O'Donnell LJ, 2017 SlicerDMRI: open source diffusion mri software for brain cancer research. Cancer Res 77, e101–e103. [PubMed: 29092950]

Pasternak O, Kelly S, Sydnor VJ, Shenton ME, 2018 Advances in microstructural diffusion neuroimaging for psychiatric disorders. Neuroimage 182, 259–282. [PubMed: 29729390]

Perrone D, Aelterman J, Pižurica A, Jeurissen B, Philips W, Leemans A, 2015 The effect of Gibbs ringing artifacts on measures derived from diffusion MRI. NeuroImage 120, 441–455. [PubMed: 26142273]

Peters BD, Dingemans PM, Dekker N, Blaas J, Akkerman E, van Amelsvoort TA, Majoie CB, den Heeten GJ, Linszen DH, de Haan L, 2010 White matter connectivity and psychosis in ultra-high-risk subjects: a diffusion tensor fiber tracking study. Psychiatry Res. 181, 44–50. [PubMed: 19954931]

Peters BD, Schmitz N, Dingemans PM, van Amelsvoort TA, Linszen DH, de Haan L, Majoie CB, den Heeten GJ, 2009 Preliminary evidence for reduced frontal white matter integrity in subjects at ultra-high-risk for psychosis. Schizophr. Res 111, 192–193. [PubMed: 19372031]

Pierpaoli C, Basser PJ, 1996 Toward a quantitative assessment of diffusion anisotropy. Magnetic Resonance Med. 36, 893–906.

Raab P, Hattingen E, Franz K, Zanella FE, Lanfermann H, 2010 Cerebral gliomas: diffusional kurtosis imaging analysis of microstructural differences. Radiology 254, 876–881. [PubMed: 20089718]

Ramani A, Jensen JH, Szulc KU, Ali O, Hu C, Lu H, Brodle JD, Helpern JA, 2007 Assessment of abnormalities in the cerebral microstructure of schizophrenia patients: a diffusional kurtosis imaging study. In: Proc. Int. Soc. Magn. Reson. Med, p. 648.

Shaw CB, Jensen JH, 2017 Recent Computational advances in denoising for magnetic resonance diffusional kurtosis imaging (DKI). J. Indian Inst. Sci 1–14.

Smith SM, Jenkinson M, Johansen-Berg H, Rueckert D, Nichols TE, Mackay CE, Watkins KE, Ciccarelli O, Cader MZ, Matthews PM, Behrens TEJ, 2006 Tract-based spatial statistics: voxelwise analysis of multi-subject diffusion data. Neuroimage 31, 1487–1505. [PubMed: 16624579]

Smith SM, Nichols TE, 2009 Threshold-free cluster enhancement: addressing problems of smoothing, threshold dependence and localisation in cluster inference. Neuroimage 44, 83–98. [PubMed: 18501637]

Steven AJ, Zhuo J, Melhem ER, 2014 Diffusion kurtosis imaging: an emerging technique for evaluating the microstructural environment of the brain. Am. J. Roentgenol 202, W26–W33. [PubMed: 24370162]

Tabesh A, Jensen JH, Ardekani BA, Helpern JA, 2011 Estimation of tensors and tensor-derived measures in diffusional kurtosis imaging. Magnetic Resonance Med. 65, 823–836.

Tang Y, Pasternak O, Kubicki M, Rathi Y, Zhang T, Wang J, Li H, Woodberry KA, Xu L, Qian Z, Zhu A, Whitfield-Gabrieli S, Keshavan MS, Niznikiewicz M, Stone WS, McCarley RW, Shenton ME, Wang J, Seidman LJ, 2019 Altered cellular white matter but not extracellular free water on diffusion MRI in individuals at clinical high risk for psychosis. Am. J. Psychiatry 176, 820–828. [PubMed: 31230461]

Thompson PM, Stein, Medland JL, Hibar SE, Vasquez DP, Renteria AA, Toro ME, Jahanshad R, Schumann N, Franke G, Wright B, Martin MJ, Agartz NG, Alda I, Alhusaini M, Almasy S, Almeida L, Alpert J, Andreasen K, Andreassen NC, Apostolova OA, Appel LG, Armstrong K, Aribisala NJ, Bastin B, Bauer ME, Bearden M, Bergmann CE, Binder O, Blangero EB, Bockholt J, Boen HJ, Bois E, Boomsma C, Booth DI, Bowman T, Bralten IJ, Brouwer J, Brunner RM, Brohawn HG, Buckner DG, Buitelaar RL, Bulayeva J, Bustillo K, Calhoun JR, Cannon VD, Cantor DM, Carless RM, Caseras MA, Cavalleri X, Chakravarty GL, Chang MM, Ching KD, Christo-forou CRK, Cichon A, Clark S, Conrod VP, Coppola P, Crespo-Facorro G, Curran B, Czisch JE, Deary M, de Geus IJ, den Braber EJC, Delvecchio A, Depondt G, de Haan C, de Zubicaray L, Dima GI, Dimitrova D, Djurovic R, Dong S, Donohoe H, Duggirala G, Dyer R, Ehrlich TD, Ekman S, Elvsåshagen CJ, Emsell T, Erk L, Espeseth S, Fagerness T, Fears J, Fedko S, Fernández I, Fisher G, Foroud SE, Fox T, Francks PT, Frangou C, Frey S, Frodl EM, Frouin T, Garavan V, Giddaluru H, Glahn S, Godlewska DC, Goldstein B, Gollub RZ, Grabe RL, Grimm HJ, Gruber O, Guadalupe O, Gur T, Gur RE, Göring RC, Hagenaars HHH, Hajek S, Hall T, Hall GB, Hardy J, Hartman J, Hass CA, Hatton J, Haukvik SN, Hegenscheid UK, Heinz K, Hickie A, Ho IB, Hoehn B-C, Hoekstra D, Hollinshead PJ, Holmes M, Homuth AJ, Hoogman G, Hong M, Hosten LE, Hottenga N, Hulshoff Pol J-J, Hwang HE, Jack KS Jr, Jenkinson CR, Jöhnston M, Jonsson C, Kahn EG, Kasperaviciute RS, Kelly D, Kim S, Kochunov S, Koenders P, Krämer L, Kwok B, Lagopoulos JBJ, Laje J, Landen G, Landman M, Lauriello BA, Lawrie J, Lee SM, Le Hellard PH, Lemaître S, Leonardo H, Li CD, Liberg C-S, Liewald B, Liu DC, Lopez X, Loth LM, Lourdusamy E, Luciano A, Macciardi M, Machielsen F, Macqueen MWJ, Malt GM, Mandl UF, Manoach R, Martinot DS, Matarin J-L, Mather M, Mattheisen KA, Mattingsdal M, Meyer-Lindenberg M, McDonald A, McIntosh C, McMahon AM, McMahon FJ, Meisenzahl KL, Melle E, Milaneschi I, Mohnke Y, Montgomery S, Morris GW, Moses DW, Mueller EK, Muñoz Maniega BA, Mühleisen S, Müller-Myhsok TW, Mwangi B, Nauck B, Nho M, Nichols K, Nilsson TE, Nugent L-G, Nyberg AC, Olvera L, Oosterlaan RL, Ophoff J, Pandolfo RA, Papalampropoulou-Tsiridou M, Papmeyer M, Paus M, Pausova T, Pearlson Z, Penninx GD, Peterson BW, Pfennig CP, Phillips A, Pike M, Poline GB, Potkin J-B, Pütz SG, Ramasamy B, Rasmussen A, Rietschel J, Rijpkema M, Risacher M, Roffman SL, Roiz-Santiañez JL, Romanczuk-Seiferth R, Rose N, Royle EJ, Rujescu NA, Ryten D, Sachdev M, Salami PS, Satterthwaite A, Savitz TD, Saykin J, Scanlon AJ, Schmaal C, Schnack L, Schork HG, Schulz AJ, Schür SC, Seidman R, Shen L, Shoemaker L, Simmons JM, Sisodiya A, Smith SM, Smoller C, Soares JW, Sponheim JC, Sprooten SR, Starr E, Steen JM, Strakowski VM, Strike S, Sussmann L, Sämann J, Teumer PG, Toga A, Tordesillas-Gutierrez AW, Trabzuni D, Trost D, Turner S, Van den Heuvel J, van der Wee M, van Eijk NJ, van Erp K, van Haren TGM, van 't Ent NEM, van Tol D, Valdés Hernández M-J, Veltman MC, Versace DJ, Völzke A, Walker H, Walter R, Wang H, Wardlaw L, Weale JM, Weiner ME, Wen MW, Westlye W, Whalley LT, Whelan HC, White CD, Winkler T, Wittfeld AM, Woldehawariat K, Wolf G, Zilles C, Zwiers D, Thalamuthu MP, Schofield A, Freimer PR, Lawrence NB, Drevets NS, Alzheimer's, W.Disease Neuroimaging Initiative, EPIGEN Consortium, IMAGEN Consortium, Saguenay Youth Study (SYS) Group, 2014 The ENIGMA Consortium: large-scale collaborative analyses of neuroimaging and genetic data. Brain Imaging Behav. 8, 153–182. [PubMed: 24399358]

Veraart J, Fieremans E, Jelescu IO, Knoll F, Novikov DS, 2016 Gibbs ringing in diffusion MRI. Magnetic Resonance Med. 76, 301–314.

Veraart J, Sijbers J, Sunaert S, Leemans A, Jeurissen B, 2013 Weighted linear least squares estimation of diffusion MRI parameters: strengths, limitations, and pitfalls. NeuroImage 81, 335–346. [PubMed: 23684865]

Wang C, Ji F, Hong Z, Poh JS, Krishnan R, Lee J, Rekhi G, Keefe RSE, Adcock RA, Wood SJ, Fornito A, Pasternak O, Chee MWL, Zhou J, 2016 Disrupted salience network functional connectivity and white-matter microstructure in persons at risk for psychosis: findings from the LYRIKS study. Psychol. Med 46, 2771–2783. [PubMed: 27396386]

Westin C-F, Knutsson H, Pasternak O, Szczepankiewicz F, Özarslan E, van Westen D, Mattisson C, Bogren M, O'Donnell LJ, Kubicki M, Topgaard D, Nilsson M, 2016 Q-space trajectory imaging for multidimensional diffusion MRI of the human brain. NeuroImage 135, 345–362. [PubMed: 26923372]

Williams EJ, 1959 Regression Analysis. wiley.

Winkler AM, Ridgway GR, Webster MA, Smith SM, Nichols TE, 2014 Permutation inference for the general linear model. Neuroimage 92, 381–397. [PubMed: 24530839]

Yang AW, Jensen JH, Hu CC, Tabesh A, Falangola MF, Helpern JA, 2012 Effect of cerebral spinal fluid suppression for diffusional kurtosis imaging. J. Magnetic Resonance Imaging 37, 365–371.

Zhang F, Breger A, Ning L, Westin C-F, O'Donnell LJ, Pasternak O, 2020a Deep learning based segmentation of brain tissue from diffusion MRI. bioRxiv, 10.1101/2020.07.30.228809.

Zhang F, Ning L, O'Donnell LJ, Pasternak O, 2019a MK-curve - characterizing the relation between mean kurtosis and alterations in the diffusion MRI signal. Neuroimage 196, 68–80. [PubMed: 30978492]

Zhang F, Noh T, Juvekar P, Frisken SF, Rigolo L, Norton I, Kapur T, Pujol S, W.W. Iii, Yarmarkovich A, Kindlmann G, Wassermann D, Estepar RSJ, Rathi Y, Kikinis R, Johnson HJ, Westin C-F, Pieper S, Golby AJ, O'Donnell ALJ, 2020b SlicerDMRI: Diffusion MRI and tractography research software for brain cancer surgery planning and visualization. JCO Clin. Cancer Inform.

Zhang F, Wu Y, Norton I, Rathi Y, Golby AJ, O'Donnell LJ, 2019b Test-retest reproducibility of white matter parcellation using diffusion MRI tractography fiber clustering. Hum. Brain Mapp 40, 3041–3057. [PubMed: 30875144]

Zhang T, Li H, Tang Y, Li H, Zheng L, Guo Q, Zhao S, Zhuo K, Qian Z, Wang L, Dai Y, Chow A, Li C, Jiang K, Wang J, Xiao Z, 2015 Screening schizotypal personality disorder for detection of clinical high risk of psychosis in Chinese mental health services. Psychiatry Res. 228, 664–670. [PubMed: 26165958]

Zhang T, Li H, Woodberry KA, Seidman LJ, Zheng L, Li H, Zhao S, Tang Y, Guo Q, Lu X, Zhuo K, Qian Z, Chow A, Li C, Jiang K, Xiao Z, Wang J, 2014 Prodromal psychosis detection in a counseling center population in China: an epidemiological and clinical study. Schizophr. Res 152, 391–399. [PubMed: 24387999]

Zheng L, Wang J, Zhang T, Li H, Li C, Jiang K, 2012 The Chinese version of the SIPS/SOPS: a pilot study of reliability and validity. Chin. Mental Health J 26, 571–576.

Zhu J, Zhuo C, Liu F, Xu L, Yu C, 2016 Neural substrates underlying delusions in schizophrenia. Sci. Rep 6, 33857. [PubMed: 27651212]

Zhu J, Zhuo C, Qin W, Wang D, Ma X, Zhou Y, Yu C, 2015 Performances of diffusion kurtosis imaging and diffusion tensor imaging in detecting white matter abnormality in schizophrenia. Neuroimage Clin 7, 170–176. [PubMed: 25610778]

Zhuo J, Xu S, Proctor JL, Mullins RJ, Simon JZ, Fiskum G, Gullapalli RP, 2012 Diffusion kurtosis as an in vivo imaging marker for reactive astrogliosis in traumatic brain injury. NeuroImage 59, 467–477. [PubMed: 21835250]
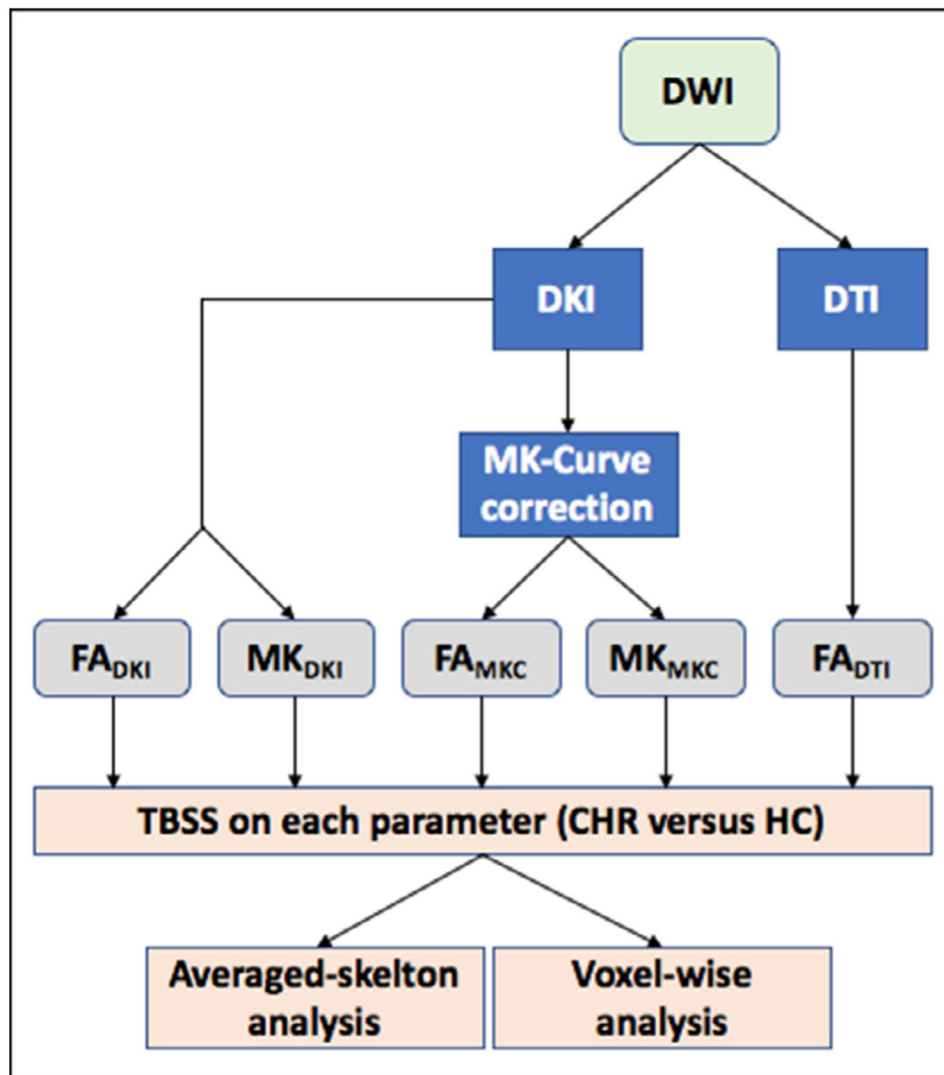
Fig. 1.
Workflow of the different outcome measures examined in this study. DTI and DKI parameters are calculated from the diffusion weighted images (DWIs). The DKI parameters also go through an MK-curve correction which eliminates implausible values. All maps are then projected on the white matter skeleton using TBSS, followed by averaged-skelton and voxel-wise analyses per parameter to study group differences between CHR and HC.
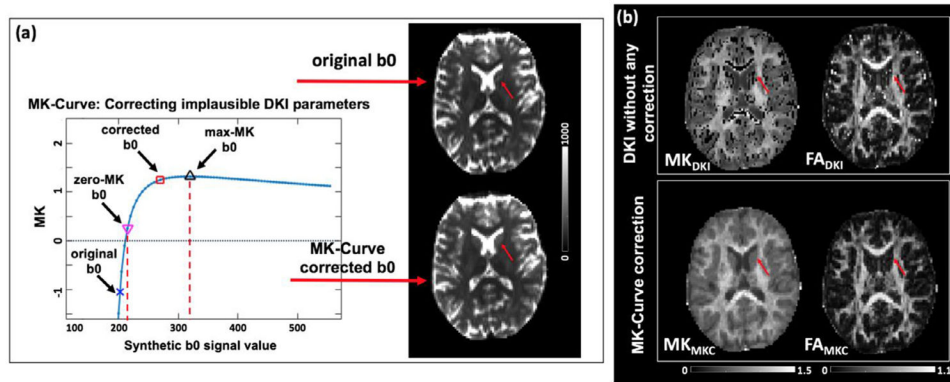
Fig. 2.
(a) A graphic illustration of the MK-Curve for an example voxel (red arrow), from which two characteristic b0 values (zero-MK b0 and max-MK b0) are calculated for identification and correction of implausible MK values. Out-of-range b0 values are projected to the plausible range by slightly modifying the b0 signals. (b) DKI parameter maps, without any correction, typically have multiple implausible values that appear as "black holes" on MK maps and very bright voxels on FA maps. The MK-curve method is able to identify and correct these values.
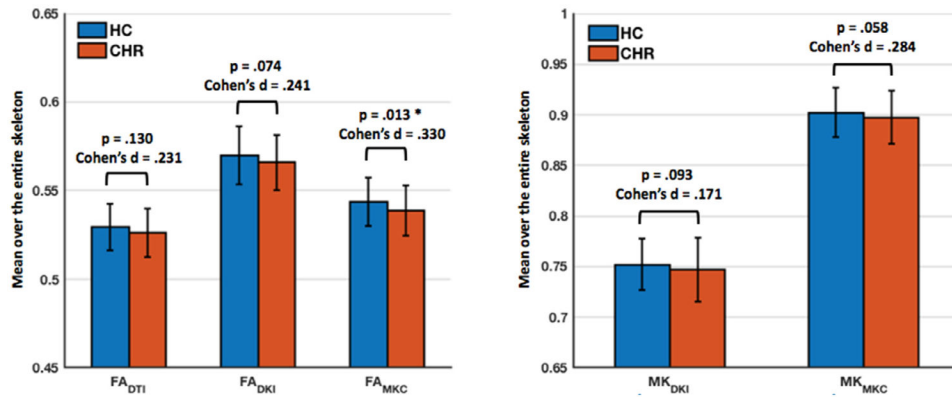
Fig. 3.
Group comparison between HC (blue) and CHR (red) of dMRI measures averaged over the whole white matter skeleton. Whiskers represent standard deviations around the mean. Following MK-curve correction, the effect sizes for group differences between HC and CHR increased, and FA_{MKC} became significantly lower in CHR compared with HC. MK-curve correction significantly decreased FA (compare FA_{DKI} with FA_{MKC}), and significantly increased MK (compare MK_{DKI} with MK_{MKC}).
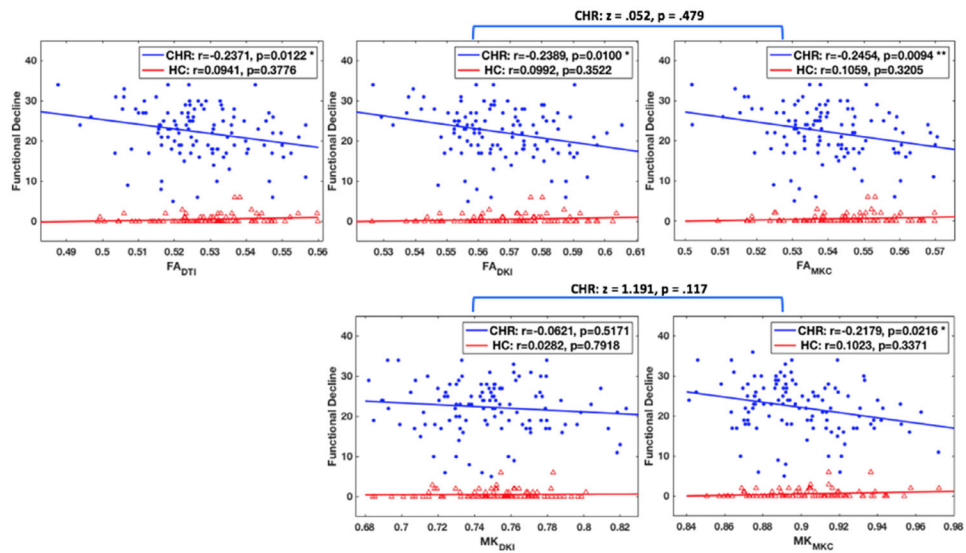
Fig. 4.
Correlation of functional decline with the average dMRI values over the whole white matter skeleton in CHR and HC. MK-curve correction increased the correlation coefficient in CHR. Although the correlation coefficients did not change significantly following MK-curve correction, MK_{MKC} became significantly correlated with Functional Decline. There were no significant correlations between dMRI measures and functional decline in HC. * indicates p < 0.05, and * * indicates p < 0.01.
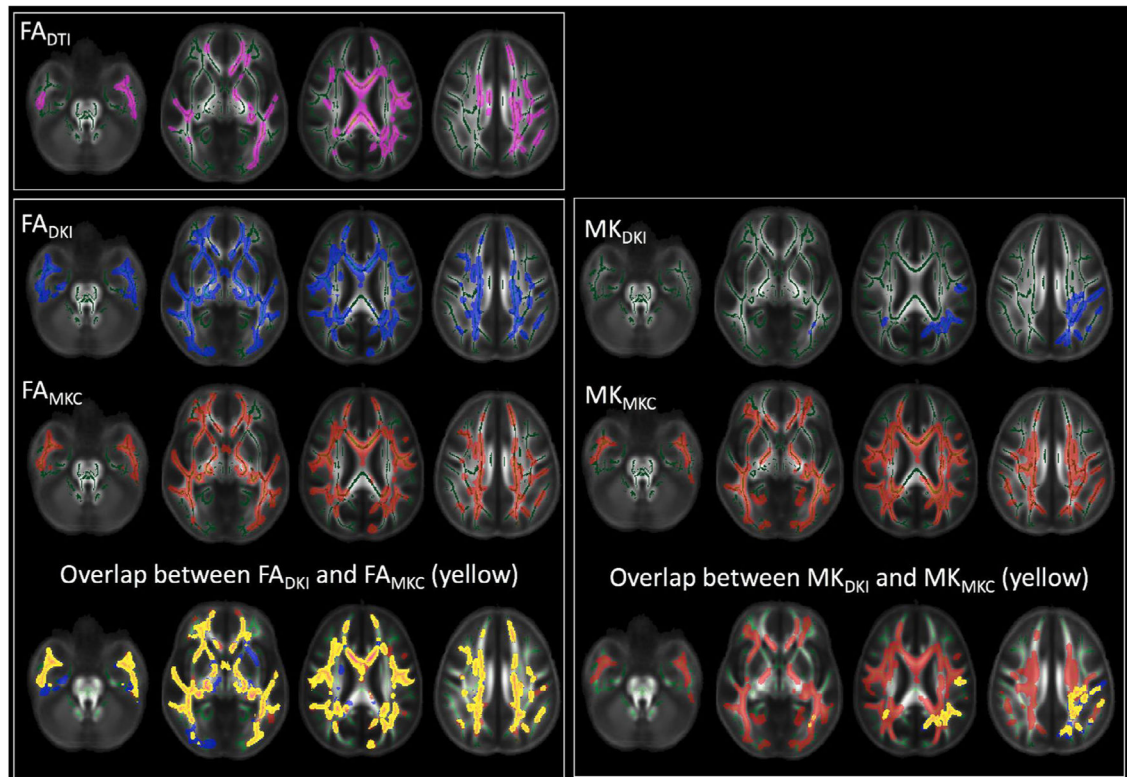
Fig. 5.
All parameters had significantly lower values in CHR compared with HC. The number of significant voxels was higher for the MK-curve corrected values (FA$_{MKC}$ and MK$_{MKC}$). While location of significant voxels highly overlapped across the FA measures, the MK$_{MKC}$ measure had many more voxels identified as lower in the CHR group than the MK$_{DKI}$ measure.

Table 1

Demographic and clinical characteristics of individuals at CHR for psychosis and HC subjects

		CHR (n = 115)	HC (n = 93)	p value
Female/male		69 / 46	44 / 49	0.09
Age		18.86 ± 4.97	18.68 ± 4.55	0.78
Education (years)		10.58 ± 2.76	10.83 ± 2.27	0.49
Global Assessment of Functioning Scale	Highest score in past 12 months	77.48 ± 4.76	79.83 ± 8.68	0.014 *
	Current score	54.63 ± 8.35	79.27 ± 8.69	< 0.001 **
Symptom measures	Positive	10.17 ± 3.47	0.42 ± 0.83	< 0.001 **
	Negative	11.21 ± 6.04	0.28 ± 0.75	< 0.001 **
	Disorganization	6.44 ± 3.37	0.32 ± 0.51	< 0.001 **
	General	9.29 ± 3.24	0.62 ± 0.96	< 0.001 **
	Overall score	37.11 ± 11.05	1.64 ± 1.88	< 0.001 **

*
p < 0.05

**
p < 0.001.

Table 2

Percentage of voxels detected to have significant group differences in voxel-wise TFCE analysis.

	FA$_{DTI}$	FA$_{DKI}$	FA$_{MKC}$	MK$_{DKI}$	MK$_{MKC}$
HC > CHR	12.70%	23.37%	26.10%	2.92%	25.79%
HC <= CHR	0%	0%	0%	0%	0%